Motivation and Preparation for the Growth of TSO/BFO Superlattices by MBE

Reid Markland,[1, a)] Maya Ramesh,[2, b)] and Darrell Schlom[2]

[1)]*Department of Physics, Auburn University*
[2)]*Department of Materials Science and Engineering, Cornell University*

As a promising room temperature multiferroic, the numerous low-energy phases of Bismuth Ferrite (BFO) are of great interest. By straining BFO layers between layers of Terbium Scandate (TSO) ground state competition arises between centrosymmetric and noncentrocymmetric phases, yielding numerous interesting properties. This paper covers the beginning phases of a project to create tri-layer BFO/TSO superlattices as a means of further exploring this complex phase dynamic.

I. INTRODUCTION

Multiferroic materials have been the focus of an explosion of research in the decades since their popularization by N. Spaldin[1]. Defined as a material simultaneously displaying coupled ferroelectric, ferromagnetic, and ferroelastic properties, multiferroics offer applications in memory storage, spintronic devices, and low-cost magnetic field control. A center-point of this research, Bismuth Ferrite (BFO) has garnered much attention in recent decades as a promising room temperature multiferroic material. In addition to having one of the strongest spontaneous polarizations per unit area known[2], BFO can take on a number of low energy phases other than its ferroelectric $R3c$ ground state when engineered with compressive[3], tensile[4], or electrostatic[5] strain.

Among the most interesting effects seen in BFO is the phase behavior of the Terbium Scandate and BFO superlattices (TSO/BFO). TSO/BFO has been shown to possess both centrosymmetric and noncentrosymmetric phases carrying respective insulating, antipolar and semiconducting, polar phases. These phases are also reversible through electric field switching, carrying promising potential application[6].

This paper will detail the beginning phases of a project to create tri-layer TSO/BFO superlattices as a means of further exploring this complex phase dynamic. Methods of BFO growth will be given followed by measurements of BFO samples grown thus far. Conclusions will include upcoming steps towards creating BFO/TSO.

II. METHODS

BFO films were grown via molecular beam epitaxy. All measurements presented were grown on (001) STO to provide a near lattice match via a relatively low-cost substrate. Growth environment consisted of 80% distilled O_3 at a pressure of $\sim$ 5e$-$6 torr over a background

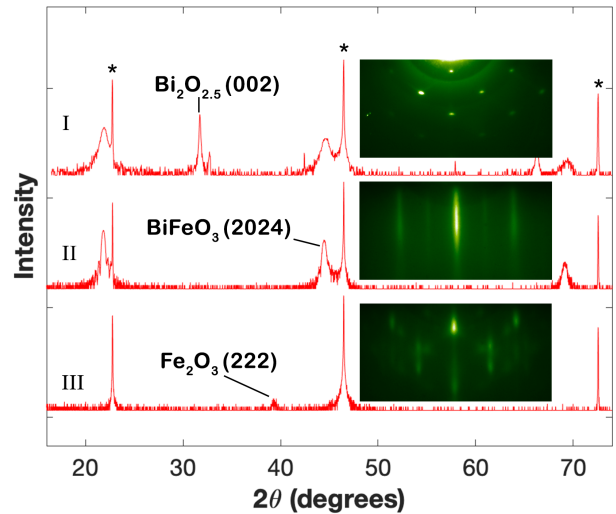[a)]rem0078@auburn.edu
[b)]mr862@cornell.edu

FIG. 1. 2θ scans of bismuth-rich BFO (I), stoichiometric BFO (II), and iron-rich BFO (III) samples. Corresponding RHEED images give *in situ* indication of material stoichiometry. Substrate peaks are indicated(*).

pressure of $\sim$ 7e$-$8 torr. O_3 was used rather than O_2 as a means of lowering oxidation pressure required while maintaining reactivity.

Due to the volatile nature of Bi, BFO was grown in an absorption controlled environment which was Fe determined. A Bi:Fe source flux ratio between 6:1 - 10:1 was maintained. The substrate temperature range best suited to growing BFO at this O_3 pressure was found to be between 650 and 700°C in close agreement with J.F. Ihlefeld et al[7].

Film stoichiometry was determined using *in situ* reflection high-energy electron diffraction (RHEED) and *ex situ* X-Ray Diffraction (XRD). The interplay between the two is depicted in Fig 1 with RHEED images depicting Bi-rich, Fe-rich, and stoichiometric BFO alongside the XRD measurements of each. Further analysis was done via piezoelectric force microscopy (PFM) in order to determine whether the BFO grown possessed ferroelectric domains.
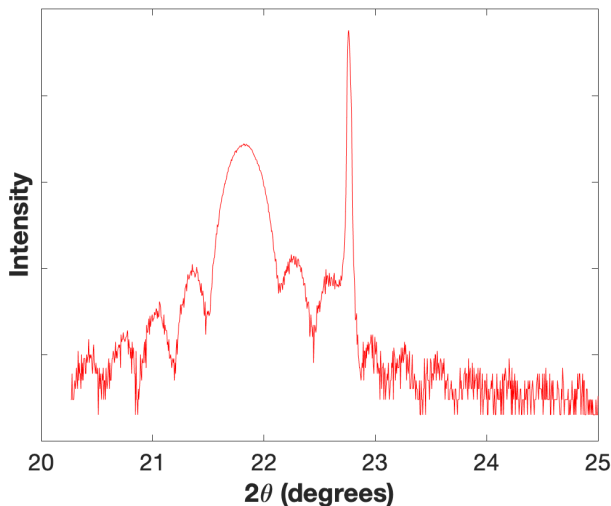
FIG. 2. 2θ scan of epitaxial BFO $30nm$ thick grown on STO substrate. Focused on the (001) substrate peak to depict high film quality.
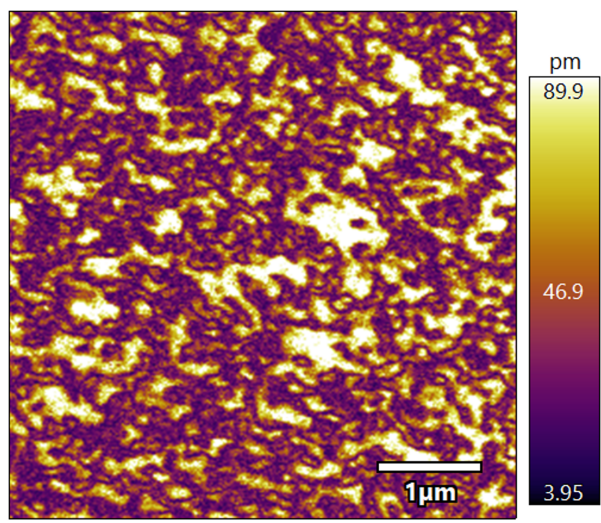

FIG. 3. PFM image of stoichiometric BFO depicting antiferroelctric $R3c$ phase. Oscillation amplitude scale depicted to the right.

III. RESULTS

After determining the bounds of the BFO growth window, several samples of stoichiometric BFO films were grown. Despite their stoichiometry, film quality needed to be improved upon as surface roughness presented an issue. A substrate temperature of $\sim 680°$C was determined to be best suited given the environment. Via AFM imaging, it was determined temperatures above $680°$C tended to result in valleys on the surface of the film, likely as a result of bismuth leaving the surface. Below $\sim 660°$C, the film displayed islands of potentially iron-rich BFO.

These nonuniformities disrupt ferroelectric effects in the BFO films, something which would prove problematic in attempting to create BFO/TSO tri-layers with clean interfaces.

The highest quality sample grown thus far is depicted in Fig. 1 as the stoichiometric BFO example (II), and is further elaborated on in Fig. 2 in a scan zoomed on the (001) STO substrate peak. The scan shows the numerous fringes of the wider perovskite peak, a clear indication of the high quality of the film. This sample was grown as an outlier, with only a 3:1 Bi:Fe flux ratio and a lower substrate temperature of $\sim 640°$C. PFM imaging of the high quality sample depicted is displayed in Fig. 3. Clear ferroelectric domains of the $R3c$ ground phase of BFO are present, another indicator of the high quality of the sample. Unfortunately, an electrode was not able to be attached thus far to test the switching voltage for such domains or derive a hysteresis loop.

IV. CONCLUSIONS

With a growth window between 650 and $700°$C, and more optimum temperature range of 660 to $680°$C, high quality BFO can be grown. While consistent growth of the quality of the presented sample has not yet been achieved, this is a simple matter of small substrate temperature, flux ratio, and perhaps O_3 pressure adjustment.

In the future, after the optimization of BFO growth, work will begin on consistent growth of high quality TSO. Once this is achieved, preparations will begin for growing BFO/TSO tri-layer superlattices. Finally, with high quality BFO/TSO superlattices, the interfacial phase behavior can be further explored.

V. ACKNOWLEDGEMENTS

[1] N. A. Hill, J. Phys. Chem. B **104**, 6694–6709 (2000).

[2] J. Seidel *et al*, Nature Materials **8**, 229–234 (2009).

[3] H. Béa *et al*, Phys. Rev. Lett. **102** (2009).

[4] J. C. Yang *et al*, Phys. Rev. Lett. **109** (2012).

[5] J. A. Mundy *et al*, Sci. Adv. **8** (2022).

[6] L. Caretta *et al*, arXiv.2201.00289 (2022).

[7] J. F. Ihlefeld *et al*, IEEE Trans. Ultrason. Ferroelecr. Freq. Control **56**, 8 (2009).